Molecular Therapy
Nucleic Acids
Original Article

CRISPR/Cas9-Mediated Treatment Ameliorates the Phenotype of the Epidermolytic Palmoplantar Keratoderma-like Mouse

Xiao-Rui Luan,[1,5] Xiao-Ling Chen,[2,5] Yue-Xiao Tang,[1,5] Jin-Yan Zhang,[1] Xiang Gao,[3] Hai-Ping Ke,[4] Zhao-Yu Lin,[3] and Xian-Ning Zhang[1]

[1]Department of Genetics, Research Center for Molecular Medicine, Institute of Cell Biology, Key Laboratory of Reproductive Genetics, Ministry of Education, Zhejiang University School of Medicine, Hangzhou, Zhejiang 310058, China; [2]Department of Biological Chemistry, Zhejiang Chinese Medical University, Hangzhou, Zhejiang 310053, China; [3]Key Laboratory of Model Animals for Disease Study of The Ministry of Education, Model Animal Research Center of Nanjing University, Nanjing, Jiangsu 210061, China; [4]Department of Biology, Ningbo College of Health Sciences, Ningbo, Zhejiang 315100, China

CRISPR/Cas9 has been confirmed as a distinctly efficient, simple-to-configure, highly specific genome-editing tool that has been used to treat monogenetic disorders. Epidermolytic palmoplantar keratoderma (EPPK) is a common autosomal dominant keratin disease resulting from dominant-negative mutation of the *KRT9* gene, and it has no effective therapy. We performed CRISPR/Cas9-mediated treatment on a knockin (KI) transgenic mouse model that carried a small indel heterozygous mutation of *Krt9*, c.434delAinsGGCT (p.Tyr144delinsTrpLeu), which caused a humanized EPPK-like phenotype. The mutation within exon 1 of *Krt9* generated a novel protospacer adjacent motif site, TGG, for Cas9 recognition and cutting. By delivering lentivirus vectors (LVs) encoding single-guide RNAs (sgRNAs) and Cas9 that targeted *Krt9* sequence into HeLa cells engineered to constitutively express wild-type and mutant keratin 9 (K9), we found the sgRNA was highly effective in reducing expression of the mutant K9 protein *in vitro*. We injected the LV into the fore-paws of adult KI-*Krt9* mice three times every 8 days and found that the expression of K9 decreased ~14.6%. The phenotypic mitigation was revealed by restoration of the abnormal differentiation and aberrant proliferation of the epidermis. Our data are the first to show that CRISPR/Cas9 is a potentially powerful therapeutic option for EPPK and other PPK subtypes.

INTRODUCTION

Hereditary palmoplantar keratoderma (PPK) is a heterogeneous group of genodermatoses characterized by abnormal thickening of the palms and soles. PPK arises from abnormal terminal differentiation and construction of the cornified envelopes.[1,2] Among the PPKs, epidermolytic PPK (EPPK; OMIM: 144200) inherited in an autosomal dominant pattern, with a worldwide incidence of 2.2–4.4 per 100,000 live newborns, is the commonest subtype. It manifests at birth or soon thereafter as diffuse yellow palmoplantar hyperkeratosis with distinct erythematous borders, sometimes combined with knuckle pads, digital mutilation, or camptodactyly. Histology may show epidermolytic areas in the upper stratum spinosum and granulosum.[1–3] Currently, dominant-negative mutations in the *KRT9* gene (encoding keratin 9 [K9]) on chromosome 17q12 are recognized as the molecular etiology in most cases.[4–8] The precise molecular and cellular abnormalities underlying EPPK remain unknown, and there is still no effective therapy 117 years after its first description by Vorner in 1901. However, the unique pathological mechanism in which EPPK is exclusively caused by dominant-negative mutations of *KRT9* makes it well suited for the development of gene-editing-based therapeutics that specifically inhibit the activity of the causative K9 allele.[2,6–8]

To date, considerable numbers of reports have confirmed that the CRISPR/Cas9 is the most innovative genome-editing technique to treat genetic defects.[7–11] In principle, CRISPR/Cas9 relies on a single-guide RNA (sgRNA) to recruit Cas9 nuclease to a specific locus by sequence complementarity and to induce double-strand breaks. These breaks are subsequently repaired either by non-homologous end joining or homology-directed repair in the presence of a donor template.[12] By introducing the CRISPR/Cas9 system into a cell line, a zygote, or a specific tissue, it is possible to ameliorate the abnormal phenotype caused by a specific disease-causing gene mutation.[11–15]

Previously, using a gene-targeting technique, we constructed a knockin (KI) transgenic mouse model that carried a small insertion-deletion (indel) heterozygous mutation of the *Krt9* gene, c.434delAinsGGCT (p.Tyr144delinsTrpLeu), corresponding to the human mutation *KRT9*/c.500delAinsGGCT (p.Tyr167delinsTrpLeu), and this caused a humanized EPPK-like phenotype.[16] The indel

Received 16 January 2018; accepted 8 May 2018;
https://doi.org/10.1016/j.omtn.2018.05.005.

[5]These authors contributed equally to this work.

Correspondence: Xian-Ning Zhang, PhD, Department of Genetics, Research Center for Molecular Medicine, Institute of Cell Biology, Key Laboratory of Reproductive Genetics, Ministry of Education, Zhejiang University School of Medicine, 866 Yuhangtang Road, Hangzhou, Zhejiang 310058, China.
E-mail: zhangxianning@zju.edu.cn

This is an open access article under the CC BY-NC-ND license (http://creativecommons.org/licenses/by-nc-nd/4.0/).

mutation within exon 1 of *Krt9* generated a novel protospacer adjacent motif (PAM) site, TGG, for Cas9 recognition and cutting. Thus, by delivering a lentivirus vector (LV) encoding sgRNAs and Cas9 that targeted the *Krt9* DNA sequence into HeLa cells engineered to constitutively express either the wild-type (WT) or the c.434delAinsGGCT mutant allele, we developed an *in vitro* cell-based system to test the CRISPR potency. We then injected LV carrying sgRNA and Cas9 components into the right fore-paw of adult KI-*Krt9* mice three times every 8 days. The phenotypic correction was demonstrated as ~14.6% reduction of disease-associated K9 after the treatment compared with controls. The mitigation of the disease was also revealed by restoration of the abnormal differentiation and aberrant proliferation of the epidermis. Our results suggested that CRISPR/Cas9 is a potentially powerful therapeutic option for EPPK and other PPK subtypes.

RESULTS

Construction of *Krt9*-Specific sgRNAs

The PAM (NGG sequence) is a critical feature of the CRISPR/Cas9 system, dictating its DNA target search mechanism.[9–11] Based on the *Krt9*/c.434delAinsGGCT mutation, a novel PAM site (TAC→TGGCTC) within exon 1 of the *Krt9* gene sequence was generated to design the sgRNA, and another novel PAM, two bases next to the mutation site, was also formed. Thus, two sgRNAs, sg1 and sg2, complementary to the sequence 20 nt adjacent to the PAM site were designed (Figure 1A). Assessed by the "Optimised CRISPR Design Tool" provided online by Dr. Feng Zhang (http://crispr.mit.edu/), sg1 and sg2 were calculated as having scores of 60 and 62, which were the highest-efficiency predictable sgRNAs that could be generated within a 10-base cut-to-mutation distance.[13] Ten potential highest-ranking genomic off-target sites in the mouse genome were also predicted using this program (Table S1).

Specificity and Potency of Lentivirus-Delivered CRISPR/Cas9 System *In Vitro*

The allele specificity and potency of sg1 and sg2 were assessed *in vitro*. We established a heterozygous HeLa cell line (HeLa Hez) stably co-expressing WT allele-mCherry and mutant (MUT) allele-EGFP, i.e., heterozygous for *Krt9* (Figure S1). HeLa Hez cells transduced by Cas9-LV without the sgRNA component served as the positive control, and cells without EGFP or mCherry fluorescence as the negative control. The fluorescence intensity of EGFP via flow cytometry (FACS) elucidated the efficacy of CRISPR/Cas9 on the target mutation sequence, and that of mCherry evaluated the possibility of off-target effects on the WT allele. Robust expression of FLAG demonstrated the transduction efficiency of LV and the high expression of Cas9, regardless of whether Cas9-LV, sg1-Cas9-LV, or sg2-Cas9-LV was transduced into cells (Figure S1).

After the transduction of sg1-Cas9-LV, potent reductions of 63.2% for total fluorescein isothiocyanate (FITC) fluorescence and 22.8% for mCherry fluorescence were observed in HeLa Hez cells, compared with lesser reductions of 32.1% and 7.0% measured in the cells infected with sg2-Cas9-LV (Figures 1B and 1C). These data indicated the specificity and potency of both sg1-Cas9-LV and sg2-Cas9-LV, but the vector sg1-Cas9-LV had a higher efficiency *in vitro* (Figure S2). The results of western blotting analysis were consistent with these observations. Using the expression levels of GAPDH and FLAG as references, we found reductions of 58.2% versus 45.8% and 43.5% versus 21.6% K9 protein in the different transduced HeLa Hez cells 72 hr after treatment, respectively (Figures 1A and 1E). Therefore, sg1-Cas9-LV was the first choice for the *in vivo* treatment.

Localized Subcutaneous Injection of the CRISPR/Cas9 System and Efficacy Assessment *In Vivo*

In the humanized EPPK-like mouse model, the phenotype developed on the major impact-dampening footpads of the main weight-bearing paws, the fore-paws. To determine whether sg1-Cas9-LV affects the process of hyperkeratosis *in vivo*, we treated 12-week-old KI-*Krt9* mice (n = 4) with subcutaneous injections of 15 μL sg1-Cas9-LV into the right fore-paw three times every 8 days, each with a viral dose of 4×10^8 infectious units/mL. The left fore-paw of the model mice was injected with Cas9-LV as controls, and all mice were imaged before and after injection. Tissues from the paw pads were analyzed by H&E staining, immunofluorescent (IF) staining, transmission electron microscopy (TEM), and immunoblotting after injection for 24 days.

The hyperpigmented calluses of the right fore-paw pad regressed significantly after treatment, compared with those of the left pad (Figure 2A). H&E staining showed that the epidermal thickness of the right pad decreased, with less expansion of the epidermis and less massive hyperkeratosis. The average epidermal thickness of the right pad was ~43 μm, half as thick as the left pad (86 μm), although it was still 1.34 times that of the normal pad of WT mice (32 μm) (Figure 2B). Usually, melanin covers the upper part of the nucleus of a keratinocyte to form a supranuclear cap to protect the nucleus from ultraviolet radiation. The melanin was increased in the epidermis of the pads of both K9 knockout and K9 mutant KI mouse models.[16,17] The results of H&E staining analysis showed reduced levels of melanin in the right pads similar to WT mice, compared with the left pads (Figure 2C).

Analysis of both IF staining and immunoblotting against FLAG reflected the higher efficiency of sg1-Cas9-LV treatment (Figure 3). The expression levels of K9 were used for normalization. Defining the K9 expression in paw pads of WT mice as 100.0%, the ratio was 140.0% in the Cas9-LV-treated left pads of KI-*Krt9* mice, but 120.0% in the sg1-Cas9-LV-treated right pads. Taking the K9 expression in the left pads of mutant mice as 100.0%, the ratio was only 71.4% for WT and 85.4% for the sg1-Cas9-LV-treated right pads of KI-*Krt9* mice, i.e., an ~14.6% decrease in K9 expression was found in the sg1-Cas9-LV-treated mice (Figure 3B). Relative to the expression level of FLAG, K9 expression was reduced 30.3% in the sg1-Cas9-LV-treated KI-*Krt9* mice (Figure 3B).

After injections for 24 days, the experimental mice were euthanized and genomic DNA (gDNA) prepared from the paw pads. PCR

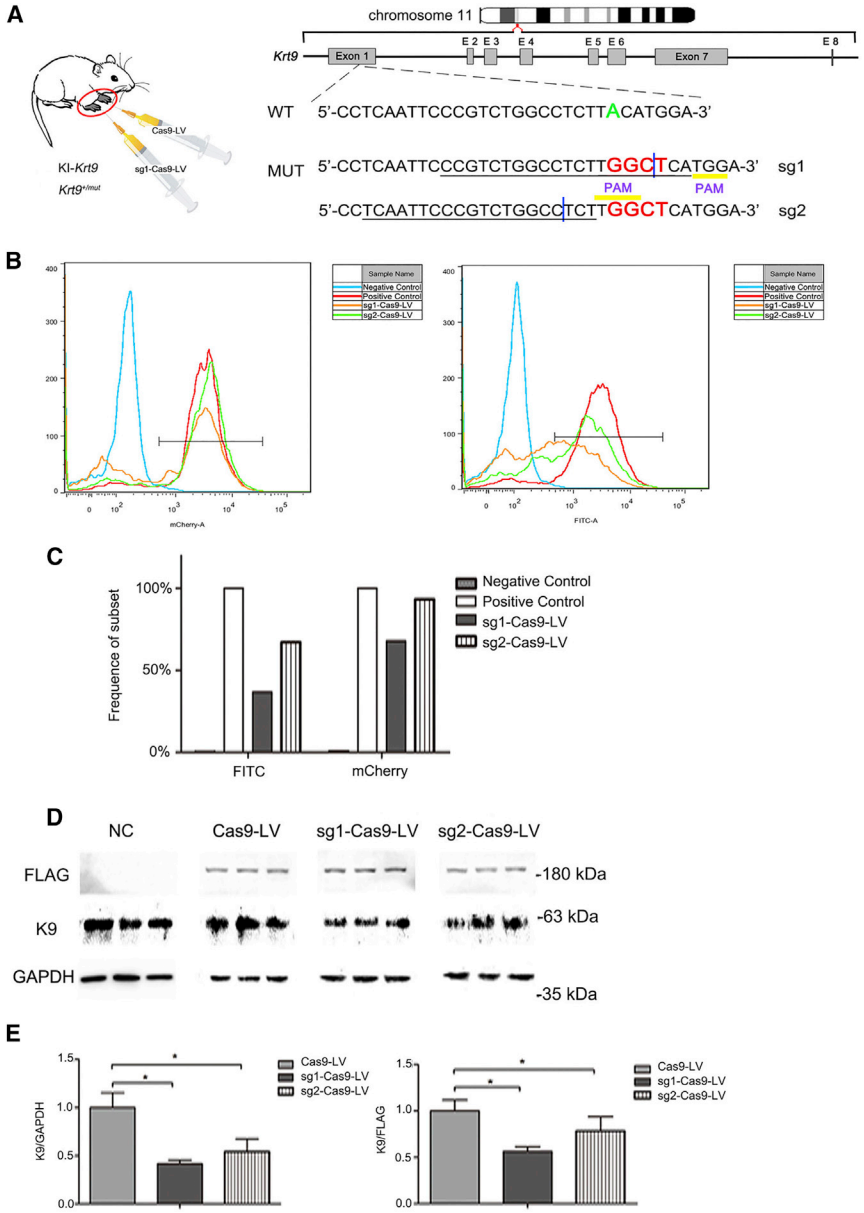

Figure 1. Delivery of CRISPR/Cas9 Mediates Gene Editing *In Vitro*

(A) Experimental design. "A" in green indicates the WT base. Two sgRNAs (underlined) were designed according to the mutation site of four bases (red in the MUT lines). PAM is indicated with yellow frame; blue vertical lines mark the cut sites. Heterozygous KI-*Krt9* mice harboring the indel mutant, c.434delAinsGGCT (p.Tyr144delinsTrpLeu), treated with sg1-Cas9-LV after *in vitro* experiments confirmed the efficacy of the LV vector. (B and C) FACS results showing the changes in FITC and mCherry fluorescence after treating HeLa cells with LV expressing both *Krt9 exon1*-EGFP and *Krt9 exon1 MUT*-mCherry (B). Thus, the HeLa Hez cell line was established. The reduction of EGFP fluorescence after transduction by sg1-Cas9-LV or sg2-Cas9-LV is shown in (C). See also Figure S2. (D and E) Immunoblotting of HeLa Hez cells against K9 (D) and semiquantitative immunoblotting analyses (relative to GAPDH and FLAG expression) (n = 3, *$p < 0.05$) (E). Each experiment was repeated at least three times. NC, untreated HeLa Hez cells; PC, HeLa Hez cells treated with Cas9-LV.

amplification targeted to the specific DNA region including exon 1 and intron 1 of *Krt9*, cloning, and Sanger sequencing were performed. In the humanized EPPK-like heterozygous mouse model, the mutant allele possessed a 121-bp KI fragment in intron 1 of *Krt9* that differentiated it from the WT allele. Both the forward and reverse sequencing results of 72 clones established from the gDNA of the sg1-Cas9-LV-treated pads identified 31 mutant clones and 41 WT clones that maintained the intact *Krt9* exon 1 and intron 1 sequence (Figure S3). DNA sequencing of the 10 potential highest-ranking genomic off-target sites in 200 clones showed only several single-nucleotide mutations at these 10 loci (Table S1). No abnormalities were observed in mice treated with either sg1-Cas9-LV or Cas9-LV.

TEM analysis revealed more normal tonofilaments and fewer cytolysis-caused vacuoles in the suprabasal layers of the epidermis of the right pads, indicating the ameliorated phenotype of KI-*Krt9* mice (Figure 4A).

IF staining against the cellular proliferation markers Ki-67 and 5-bromo-2′-deoxyuridine (BrdU) and the keratinocyte differentiation markers involucrin and filaggrin demonstrated the partial rescue of abnormal proliferation after the sg1-Cas9-LV injection. Ki-67 is an excellent marker to determine the growth fraction of a given cell population (Figure 4B). BrdU, a thymidine analog that is incorporated into dividing cells during DNA synthesis, was also used to measure cell proliferation, and the data supported the result of Ki-67 staining (Figure S4).[18] Although both involucrin and filaggrin appropriately localized to the granular layer in WT mice, we observed a decrease of involucrin and filaggrin staining intensity within the horny layer of the treated KI-Krt9 mice (Figure 4B).

In the paw pads of KI-*Krt9* mice, the dominant-negative mutation of K9 induces an imbalance in a subset of palmoplantar keratins (K1, K2, K5, K6, K10, K14, and K16).[16] After sg1-Cas9-LV treatment, the results of both immunoblotting and IF staining showed that both the expression levels and localization of these keratins were rescued and similar to those in WT mice (Figure 5). Among them, the expression of K2 increased 48.9%; K6, 43.2%; K14, 19.7%, and K16, 28.9% (Figure 5B). Significant changes in the expression and localization of K1 and K14 were similar to those in WT mice, which also indicated

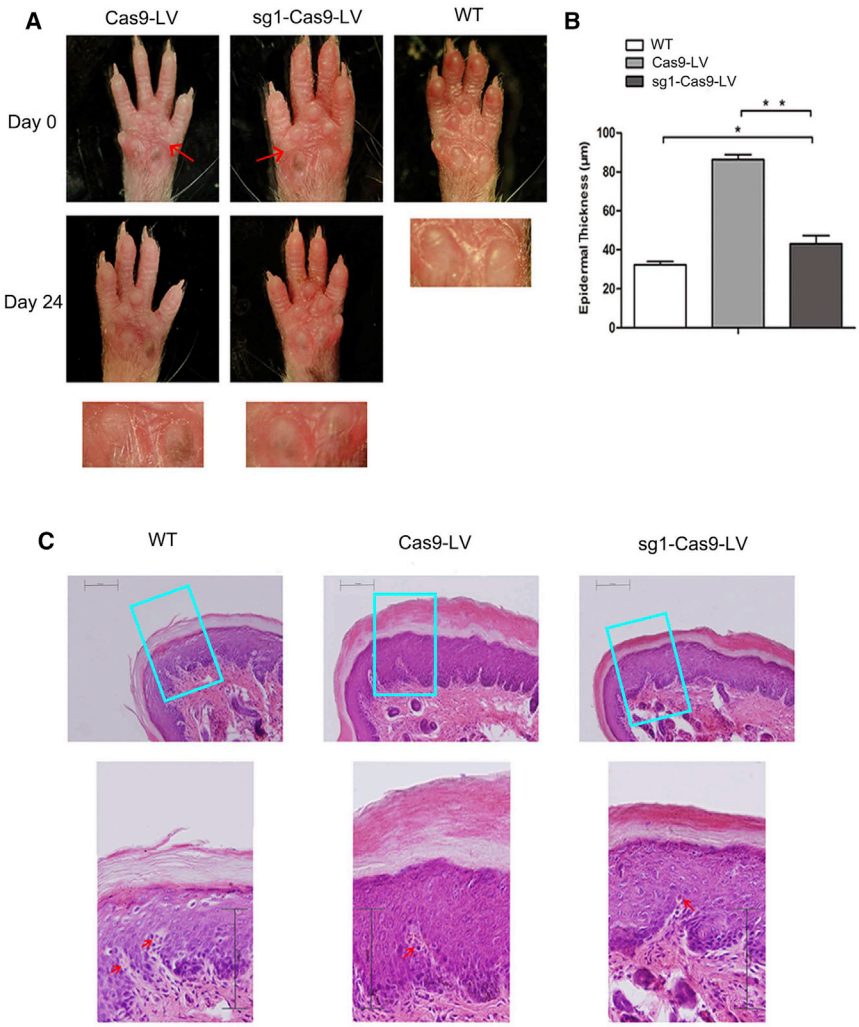

Figure 2. Fore-Paw Pad Abnormalities Are Partly Rescued in the sg1-Cas9-LV-Treated Adult KI-*Krt9* Mouse

(A) Fore-paw pads of KI-*Krt9* mice treated with Cas9-LV or sg1-Cas9-LV, and those of untreated WT mice. Red arrows indicate injection locations of Cas9-LV and sg1-Cas9-LV. (B) Analysis of epidermal thickness from the pads. (C) Representative images of H&E-stained epidermis showing that melanin (red arrows) and epidermal thickness decreased after sg1-Cas9-LV treatment. Each experiment was repeated at least three times. Scale bars, 100 μm. Mean ± SEM. *$p < 0.05$; **$p < 0.01$.

that the differentiation of epidermis treated with sg1-Cas9-LV tended toward the normal state (Figure 5C).

DISCUSSION

The vast majority of mutations in inherited keratin disorders are either missense or small in-frame indel mutations, and the disease severity is often related to the position of the mutation. The dominant-negative mutant K9 protein interferes with the function of the normal allele. The treatment challenge is to specifically decrease the expression or impact of the mutant allele or its encoded mutant protein without disrupting the expression or function of the normal allele or its normal protein. Thus, the *Krt9*/c.434delAinsGGCT (p.Tyr144delinsTrpLeu) KI mouse is an excellent heterozygous model for gene therapy research.[16] To the best of our knowledge, this study is the first to report CRISPR/Cas9 system delivery by LV, leading to *in vivo* gene therapy amelioration of the disease phenotype in a humanized EPPK-like mouse model.

Designing the optimal sgRNA is crucial for the CRISPR/Cas9 system to target a specific site in the genome, especially when the target site only has several bases different from the other DNA sequences. PAM-site mutations seem broadly effective, so sgRNA target mutations may have variable effects at different loci.[19] Here, our data demonstrated that the sgRNA with the cut-site mutation (sg1) was more efficient than that with the PAM-site mutation (sg2) (Figures 1B and 1C).

Relative to FLAG and GAPDH, the reduction of K9 differed by 13.2% between *in vitro* and *in vivo* using semiquantitative analyses of immunoblotting (Figures 1D, 1E, 3B, and 3C). Because the expression of FLAG was positively correlated with the transduction efficiency of LV, this difference may be caused by disparities between the internal environment and *in vitro*. There may be some other regulatory pathways impacting the expression of K9 in the mouse. Although the efficiency of the CRISPR/Cas9 system has been evaluated on *KRT12* by plasmid, on *KRT14* in cells, and on recessive dystrophic epidermolysis bullosa cells from a patient's skin biopsy and an embryo, no evaluation with a highly efficient vector *in vivo* has been carried out on genodermatoses.[20–23] Thus, the difference in efficiency between *in vitro* and *in vivo* should be considered when further CRISPR/Cas9 therapy is applied *in vivo*.

RNAi therapy has been used on humans with pachyonychia congenita, a genodermatosis with an autosomal dominant transmission that includes a disabling plantar keratoderma.[24] During 100 days of treatment with 33 rounds of injections, clearing of the callus around the site of injection developed, but the level of pain during the injections is a significant concern, and the effect may not persist.[24] Unlike the RNAi method, CRISPR/Cas9 targets DNA rather than RNA, ensuring that the effect is permanent.[25] Compared with our previous shRNA therapy delivered by LV in the same *Krt9*/KI mouse model, the reduction of thickness of treated pads by the CRISPR/Cas9 system was 10% greater.[16] Because CRISPR/Cas9 is derived from prokaryotes, it has less crosstalk with eukaryotic components than the RNAi pathway.[9] The higher specificity of CRISPR/Cas9 may allow for fewer injections

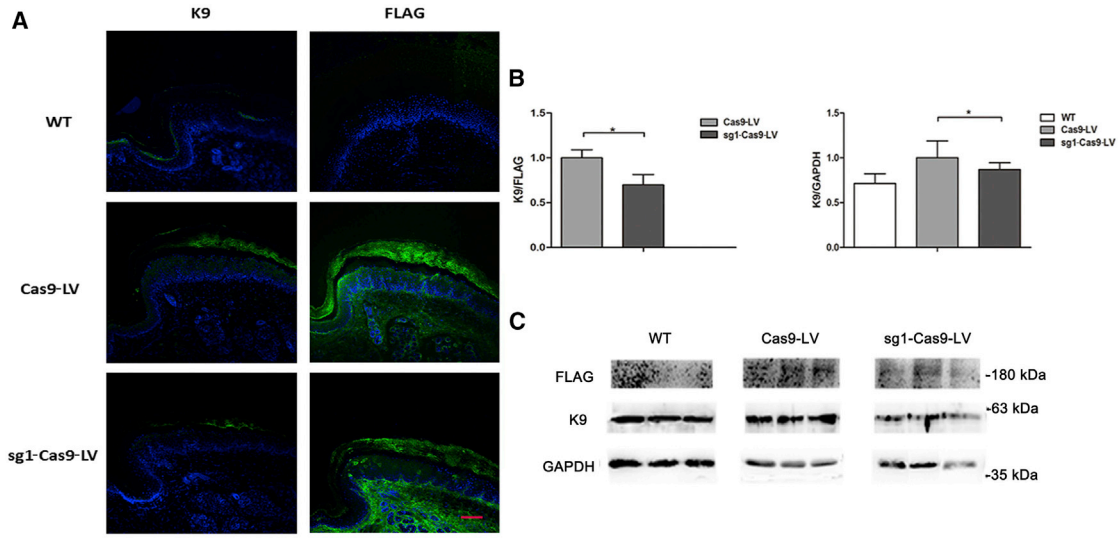

Figure 3. Delivery of sg1-Cas9-LV Decreases the Excessive Expression of K9

(A) IF staining against K9 and FLAG. Scale bar, 50 μm. (B) Semiquantitative immunoblotting analyses relative to GAPDH and FLAG (mean ± SEM; n = 3; *p < 0.05). (C) Immunoblotting against K9, GAPDH, and FLAG. Each experiment was repeated at least three times.

than RNAi therapy.[9,26] Because there are still no treatments for EPPK, the CRISPR/Cas9 system could provide an option for clinical trials.

Most researchers use adeno-associated virus (AAV) as a tool to deliver the CRISPR/Cas9 components. From the efforts reflected by the 2,463 clinical trials that have been conducted to date, 183 used AAV vectors and 158 used LV vectors in the gene therapy (October 2017; https://www.wiley.com/legacy/wileychi/genmed/clinical/). In contrast, LVs belong to the class of retroviruses that includes HIV, and are capable of DNA integration in non-dividing cells, including neurons.[27,28] Not showing preferential integration into any specific gene locus, LVs can thus reduce the chances of activating an oncogene in a large number of cells.[29] In addition, LVs have a larger cargo capacity and a more stable long-term transgene expression than AAVs, which allows expression of the larger Cas9 proteins, enabling the targeting of more genomic sites.[30,31] So far, only a few studies have demonstrated *in vivo* gene editing following LV delivery of Cas9.[31–34] In this study, we chose LV as the delivery tool and suggested a better therapeutic efficacy over the renewal cycle of the epidermis. Then, the disrupted cytoskeletal integrity, abnormal differentiation, and irregular proliferation were ameliorated. Thus, we suggest that the CRISPR/Cas9-mediated genome editing tool is an effective means of gene modification in the epidermis and a therapeutic approach to correcting defective proteins.

The off-target effect is still of great concern for application of CRISPR/Cas9-mediated genome engineering.[35] Rare "off-target" effects of a protein can be caused by DNA mutations in off-target genes and contribute to the development of certain human tumors.[36] Identifying off-target cleavage is a formidable problem given the size and complexity of the eukaryotic genome.[37] In this study, in the 49 potential highest-ranking genomic off-target sites predicted by the "Optimised CRISPR Design Tool" (Table S1), several off-target sites were located within the exons of functional genes, while only the top 24 of these sites were expressed in skin. The results of DNA sequencing from gDNA clones showed that the mismatched rate among the 10 potential highest ranking genomic off-target sites was only 3/200, indicating that there were no notable off-target effects (Table S2).

The CRISPR/Cas9 system has been widely used in spermatogonial stem cells, in various mouse models of human genetic disorders, and even in even age-related macular degeneration.[38–42] There are 10 clinical trials under investigation based on the strategy of CRISPR/Cas9 (https://clinicaltrials.gov), two of which focus on the safety of CRISPR-Cas9. Although therapeutic safety and efficacy after transplantation remain to be evaluated clinically, CRISPR/Cas9-mediated treatment provides a new vision of cell therapy for many genetic diseases.[26]

After the genomic changes occur following the transduction of the CRISPR/Cas9 system, using cytokines as adjuvant therapy to accelerate regeneration could be a feasible means of enhancing the therapeutic efficacy.[43,44] Unlike the general therapeutic strategies for genetic diseases targeting either the genetic cause underlying a specific disorder or disease-specific pathophysiological pathways, the current standard care for EPPK and other keratin disorders still only has retinoids for treating the hyperkeratosis, focusing on symptomatic treatment. Although the CRISPR/Cas9 system had a significant effect on adult *Krt9*/KI mice after local injection, we predict that this therapy could be more effective with adjuvant treatment.

In conclusion, our research demonstrates the therapeutic benefits of LV-mediated CRISPR/Cas9 genome editing in an adult mouse model of EPPK, indicating that localized injection of the CRISPR/Cas9 system is a potentially powerful treatment for genetic defects that have local effects, such as hereditary PPKs.

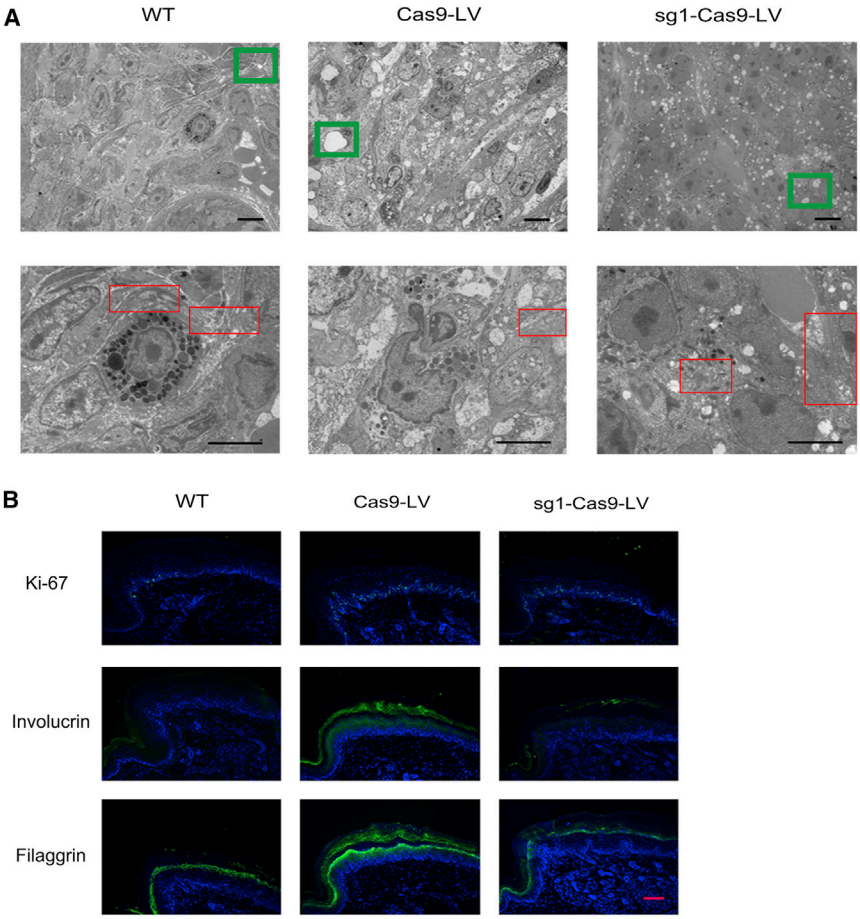

Figure 4. Disrupted Cytoskeletal Integrity and Abnormal Proliferation Are Inhibited

(A) Ultrastructural images showing the form of tonofilaments (red frames), cytolysis (green frames), and keratin filaments. Scale bars, 5 μm. (B) IF staining against Ki-67, involucrin, and filaggrin after treatment. Each experiment was repeated at least three times. Scale bar, 50 μm.

MATERIALS AND METHODS

Construction of Lentiviral Delivery for CRISPR/Cas9

Construction of the lentiviral delivery systems Cas9-LV, sg1-Cas9-LV, and sg2-Cas9-LV was based on the vector GV392. The EGFP fragment was replaced with the expression sequence FLAG. The sg1 strand *5′-CACCGCCGTCTGGCCTCTTGGCTCA-3′* and the sg2 strand *5′-CACCGTCAATTCCCGTCTGGCCTCT-3′* were synthesized by GeneChem (Shanghai, China). The Cas9-LV vector had no sgRNA strand.

Cell Culture and Transduction of HeLa Cells with Lentiviral Vectors

LVs containing *Krt9 exon1 MUT*-EGFP and *Krt9 exon1*-mCherry were produced as follows: 24 hr after plating, 293FT cells were co-transfected with 1.0 μg of *Krt9 exon1 MUT*-eGF or *Krt9 exon1*-mCherry (Figure S1A), 0.75 μg of psPAX2 (#VT1444; YouBio, Hunan, China), and 0.25 μg of pMD2.G (#VT1443; YouBio, Hunan, China) using Lipofectamine 2000 (#11668-019; Invitrogen). After incubation for 48 hr, the medium was replaced with fresh medium. The supernatant was collected, and reconstructed LVs were harvested by centrifugation and stored at −80°C for further experiments. HeLa cells were transduced with the two reconstructed LVs. After selection of cells expressing double fluorescence using BD FACSAria III (Becton Dickinson, Franklin Lakes, NJ, USA), a stable HeLa Hez cell line was established. Then, HeLa Hez cells were infected with CRISPR/Cas9-LV (1×10^7 infectious units/mL) at a dose of 10 μL for 3–5 $\times$ 10^2 cells. The cells were cultured at 37°C with 5% (v/v) CO_2 and the medium replaced every 12 hr.

Flow Cytometry

The cells were prepared for FACS 60 hr after replacing the medium. Before FACS, the cells were suspended in PBS, pipetted, and filtered. The BD FACSAria III was operated using the standard protocol. Analysis was performed using FlowJo software.

Western Blotting

Epidermis from the fore-paw pads of WT and KI-*Krt9* littermates was dissected and ground in liquid nitrogen. The next steps were the same for both cells and tissues. Radioimmunoprecipitation assay (RIPA) buffer (0.5% Nonidet P-40 [NP-40], 1% SDS, 50 mM Tris [pH 8.0], 0.1 mM EDTA, 150 mM NaCl, 100 μM Na_3VO_4, 1 mM dithiothreitol, 0.4 mM phenylmethylsulfonyl fluoride, 3 μg/mL aprotinin, 2 μg/mL pepstatin, 1 μg/mL leupeptin) was used to lyse cells and tissues. The mixture was then centrifuged at 4°C for 20 min. After adding 4× loading buffer, the protein sample was denatured for 5 min at 95°C. The gel was run at 120 V for 90 min. After blotting the protein onto polyvinylidene fluoride membranes, the membranes were blocked for 60 min in skim milk and incubated overnight at 4°C with the primary antibody. The membranes were washed and incubated with the secondary antibody for 60 min. The bound antibodies were visualized with the Tanon 5200 chemiluminescent imaging system (Biotanon, Shanghai, China). The results of staining per area were generated by ImageJ with t test statistical analysis.

Animals

Mice on a *C57BL/6* genetic background carrying *Krt9*/c.434delAinsGGCT were housed in groups with a 12-hr dark/light cycle and free access to food and water in accordance with the Regulations on Mouse Welfare and Ethics of Nanjing University, China. All procedures were conducted with the approval of Model Animal Research Center of Nanjing University. Mice between 12 and 16 weeks of age were used in all experiments.[16]

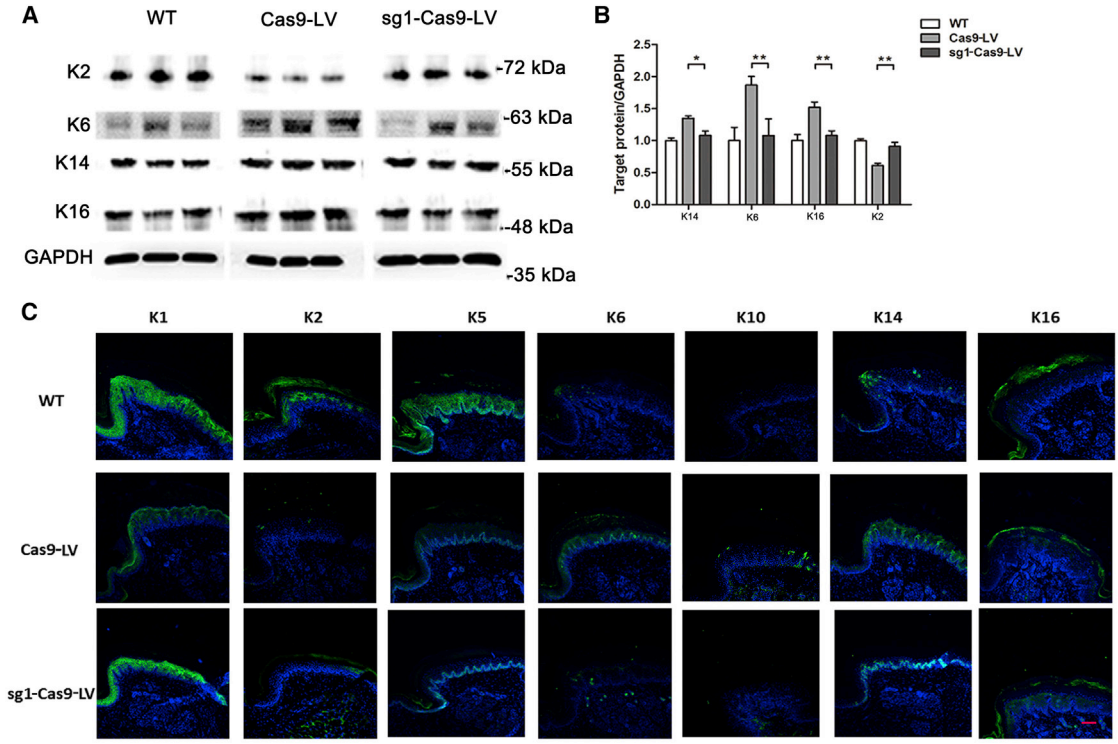

Figure 5. CRISPR/Cas9-Mediated Therapy Improves the Compensatory Expression of Other Palmoplantar Keratins

(A) Immunoblotting against K2, K6, K14, and K16. (B) Semiquantitative immunoblotting analyses relative to GAPDH (mean ± SEM; n = 3; *$p < 0.05$; **$p < 0.01$). (C) IF staining for K1, K2, K5, K6, K10, K14, and K16. Each experiment was repeated at least three times. Scale bar, 50 μm.

Localized Subcutaneous Injection

Mice were anesthetized by an intraperitoneal injection of chloral hydrate (40 mg/g). Localized subcutaneous injections of sg1-Cas9-LV into the right fore-paws of mice were performed using a microsyringe (location of injection is shown in Figure 2A).

BrdU Incorporation Assay

Each mouse received an intraperitoneal injection of 200 mg/kg BrdU twice every 1.5 hr, and epidermis from the fore-paw pads was dissected 2 hr after the second injection. BrdU (BrdU powder, No. E607203; Sangon Biotech, Shanghai, China) was prepared in PBS.

Histopathology and Immunofluorescence Analysis

Epidermis from the fore-paw pads of WT and KI-*Krt9* littermates was dissected and fixed at 4°C for 4 hr in 4% paraformaldehyde/PBS. Then the tissues were dehydrated, embedded in paraffin, and cut at 8 μm. For histopathological analyses, the sections were deparaffinized and stained with H&E using standard protocols. Epidermal thickness was measured with t test statistical analysis using Photoshop software. For IF analysis, rehydrated paraffin-embedded sections were washed in PBS, blocked in 5% normal goat serum for 1 hr at room temperature, incubated with primary antibody (in 2.5% normal goat serum) at 4°C for 16 hr overnight, incubated with secondary antibody (in 2.5% normal goat serum) for 45 min, counterstained with DAPI, mounted, and imaged (the sections were washed three times in PBS before each step). Images were captured using a Leica SP5 Laser Scanning Confocal Microscope (Leica, Buffalo, IL, USA).

TEM and Barrier Function Assays

For TEM, tissues from the footpads of fore-paws were fixed in 2.5% glutaraldehyde in cacodylate buffer for 24 hr at 4°C. After rinsing twice with cacodylate buffer, samples were post-fixed in aqueous osmium tetroxide for 2 hr at 20°C. Samples were rinsed three times with cacodylate buffer and dehydrated through a graded series of ethanol concentrations. After dehydration through acetone, samples were infiltrated with complete embedding medium and dried in a 60°C oven for 48 hr. Then, the samples were cut at 70 nm and stained with 2% uranium acetate-saturated alcohol and lead citrate for 15 min each. Ultra-thin sections were examined on a TEM (HT7700; Hitachi, Tokyo, Japan).

T-A Cloning

To investigate the nature and frequency of the specific sg1-Cas9-LV-corrected indel, we performed T-A cloning and Sanger sequencing analysis using PCR amplicons from the gDNA at *Krt9* exon 1 and 10 different loci. Epidermis from the fore-paw pads of WT and KI-*Krt9* littermates treated with Cas9-LV or sg1-Cas9-LV was sampled for gDNA extraction. Then, PCR, T-A cloning (pMD 18-T Vector Cloning Kit, #6011; TaKaRa, Shiga, Japan), and Sanger sequencing were carried out according to standard protocols.

SUPPLEMENTAL INFORMATION

Supplemental Information includes four figures and two tables and can be found with this article online at https://doi.org/10.1016/j.omtn.2018.05.005.

AUTHOR CONTRIBUTIONS

Writing – Original Draft, X.-R.L., X.-L.C., and Y.-X.T.; Writing – Reviewing and Editing, X.-R.L., X.-L.C., Y.-X.T., J.-Y.Z., H.-P.K., Z.-Y.L., and X.-N.Z.; Supervision, X.G., H.-P.K., Z.-Y.L., and X.-N.Z.; Investigation, X.-R.L., X.-L.C., Y.-X.T., J.-Y.Z., and H.-P.K.; Methodology, X.-R.L., X.-L.C., Y.-X.T., and Z.-Y.L.

CONFLICTS OF INTEREST

The authors have no conflict of interest.

ACKNOWLEDGMENTS

This study was supported by the National Natural Science Foundation of China (81450065), research funding of Zhejiang Chinese Medical University (711200F011), and the Ningbo Natural Science Foundation (2015A610187).

REFERENCES

1. Sybert, V.P. (2017). Genetic Skin Disorders, Third Edition (Oxford University Press), pp. 34–53.
2. Has, C., and Technau-Hafsi, K. (2016). Palmoplantar keratodermas: clinical and genetic aspects. J. Dtsch. Dermatol. Ges. *14*, 123–139, quiz 140.
3. Lopez-Valdez, J., Rivera-Vega, M.R., Gonzalez-Huerta, L.M., Cazarin, J., and Cuevas-Covarrubias, S. (2013). Analysis of the KRT9 gene in a Mexican family with epidermolytic palmoplantar keratoderma. Pediatr. Dermatol. *30*, 354–358.
4. Reis, A., Hennies, H.C., Langbein, L., Digweed, M., Mischke, D., Drechsler, M., Schröck, E., Royer-Pokora, B., Franke, W.W., Sperling, K., et al. (1994). Keratin 9 gene mutations in epidermolytic palmoplantar keratoderma (EPPK). Nat. Genet. *6*, 174–179.
5. Du, Z.F., Wei, W., Wang, Y.F., Chen, X.L., Chen, C.Y., Liu, W.T., Lu, J.J., Mao, L.G., Xu, C.M., Fang, H., and Zhang, X.N. (2011). A novel mutation within the 2B rod domain of keratin 9 in a Chinese pedigree with epidermolytic palmoplantar keratoderma combined with knuckle pads and camptodactyly. Eur. J. Dermatol. *21*, 675–679.
6. McLean, W.H., and Moore, C.B. (2011). Keratin disorders: from gene to therapy. Hum. Mol. Genet. *20* (R2), R189–R197.
7. Coulombe, P.A. (2017). The molecular revolution in cutaneous biology: keratin genes and their associated disease: diversity, opportunities, and challenges. J. Invest. Dermatol. *137*, e67–e71.
8. March, O.P., Reichelt, J., and Koller, U. (2018). Gene editing for skin diseases: designer nucleases as tools for gene therapy of skin fragility disorders. Exp. Physiol. *103*, 449–455.
9. Long, C., Amoasii, L., Mireault, A.A., McAnally, J.R., Li, H., Sanchez-Ortiz, E., Bhattacharyya, S., Shelton, J.M., Bassel-Duby, R., and Olson, E.N. (2016). Postnatal genome editing partially restores dystrophin expression in a mouse model of muscular dystrophy. Science *351*, 400–403.
10. Eyquem, J., Mansilla-Soto, J., Giavridis, T., van der Stegen, S.J., Hamieh, M., Cunanan, K.M., Odak, A., Gönen, M., and Sadelain, M. (2017). Targeting a CAR to the TRAC locus with CRISPR/Cas9 enhances tumour rejection. Nature *543*, 113–117.
11. Gulei, D., and Berindan-Neagoe, I. (2017). CRISPR/Cas9: a potential life-saving tool. What's next? Mol. Ther. Nucleic Acids *9*, 333–336.
12. Ormond, K.E., Mortlock, D.P., Scholes, D.T., Bombard, Y., Brody, L.C., Faucett, W.A., Garrison, N.A., Hercher, L., Isasi, R., Middleton, A., et al. (2017). Human germline genome editing. Am. J. Hum. Genet. *101*, 167–176.
13. Hsu, P.D., Lander, E.S., and Zhang, F. (2014). Development and applications of CRISPR-Cas9 for genome engineering. Cell *157*, 1262–1278.
14. Dai, W.J., Zhu, L.Y., Yan, Z.Y., Xu, Y., Wang, Q.L., and Lu, X.J. (2016). CRISPR-Cas9 for in vivo gene therapy: promise and hurdles. Mol. Ther. Nucleic Acids *5*, e349.
15. Yin, H., Song, C.Q., Dorkin, J.R., Zhu, L.J., Li, Y., Wu, Q., Park, A., Yang, J., Suresh, S., Bizhanova, A., et al. (2016). Therapeutic genome editing by combined viral and non-viral delivery of CRISPR system components in vivo. Nat. Biotechnol. *34*, 328–333.
16. Lyu, Y.S., Shi, P.L., Chen, X.L., Tang, Y.X., Wang, Y.F., Liu, R.R., Luan, X.R., Fang, Y., Mei, R.H., Du, Z.F., et al. (2016). A small indel mutant mouse model of epidermolytic palmoplantar keratoderma and its application to mutant-specific shRNA therapy. Mol. Ther. Nucleic Acids *5*, e299.
17. Fu, D.J., Thomson, C., Lunny, D.P., Dopping-Hepenstal, P.J., McGrath, J.A., Smith, F.J.D., Irwin McLean, W.H., and Leslie Pedrioli, D.M. (2014). Keratin 9 is required for the structural integrity and terminal differentiation of the palmoplantar epidermis. J. Invest. Dermatol. *134*, 754–763.
18. Wojtowicz, J.M., and Kee, N. (2006). BrdU assay for neurogenesis in rodents. Nat. Protoc. *1*, 1399–1405.
19. Paquet, D., Kwart, D., Chen, A., Sproul, A., Jacob, S., Teo, S., Olsen, K.M., Gregg, A., Noggle, S., and Tessier-Lavigne, M. (2016). Efficient introduction of specific homozygous and heterozygous mutations using CRISPR/Cas9. Nature *533*, 125–129.
20. Courtney, D.G., Moore, J.E., Atkinson, S.D., Maurizi, E., Allen, E.H., Pedrioli, D.M., McLean, W.H., Nesbit, M.A., and Moore, C.B. (2016). CRISPR/Cas9 DNA cleavage at SNP-derived PAM enables both in vitro and in vivo KRT12 mutation-specific targeting. Gene Ther. *23*, 108–112.
21. Kocher, T., Peking, P., Klausegger, A., Murauer, E.M., Hofbauer, J.P., Wally, V., Lettner, T., Hainzl, S., Ablinger, M., Bauer, J.W., et al. (2017). Cut and paste: efficient homology-directed repair of a dominant negative KRT14 mutation via CRISPR/Cas9 nickases. Mol. Ther. *25*, 2585–2598.
22. Hainzl, S., Peking, P., Kocher, T., Murauer, E.M., Larcher, F., Del Rio, M., Duarte, B., Steiner, M., Klausegger, A., Bauer, J.W., et al. (2017). COL7A1 editing via CRISPR/Cas9 in recessive dystrophic epidermolysis bullosa. Mol. Ther. *25*, 2573–2584.
23. Wu, W., Lu, Z., Li, F., Wang, W., Qian, N., Duan, J., Zhang, Y., Wang, F., and Chen, T. (2017). Efficient in vivo gene editing using ribonucleoproteins in skin stem cells of recessive dystrophic epidermolysis bullosa mouse model. Proc. Natl. Acad. Sci. USA *114*, 1660–1665.
24. Leachman, S.A., Hickerson, R.P., Schwartz, M.E., Bullough, E.E., Hutcherson, S.L., Boucher, K.M., Hansen, C.D., Eliason, M.J., Srivatsa, G.S., Kornbrust, D.J., et al. (2010). First-in-human mutation-targeted siRNA phase Ib trial of an inherited skin disorder. Mol. Ther. *18*, 442–446.
25. Morgens, D.W., Deans, R.M., Li, A., and Bassik, M.C. (2016). Systematic comparison of CRISPR/Cas9 and RNAi screens for essential genes. Nat. Biotechnol. *34*, 634–636.
26. Yin, H., Song, C.Q., Suresh, S., Wu, Q., Walsh, S., Rhym, L.H., Mintzer, E., Bolukbasi, M.F., Zhu, L.J., Kauffman, K., et al. (2017). Structure-guided chemical modification of guide RNA enables potent non-viral in vivo genome editing. Nat. Biotechnol. *35*, 1179–1187.
27. Cavazzana-Calvo, M., Payen, E., Negre, O., Wang, G., Hehir, K., Fusil, F., Down, J., Denaro, M., Brady, T., Westerman, K., et al. (2010). Transfusion independence and HMGA2 activation after gene therapy of human β-thalassaemia. Nature *467*, 318–322.
28. Palfi, S., Gurruchaga, J.M., Ralph, G.S., Lepetit, H., Lavisse, S., Buttery, P.C., Watts, C., Miskin, J., Kelleher, M., Deeley, S., et al. (2014). Long-term safety and tolerability of ProSavin, a lentiviral vector-based gene therapy for Parkinson's disease: a dose escalation, open-label, phase 1/2 trial. Lancet *383*, 1138–1146.
29. Kotterman, M.A., Chalberg, T.W., and Schaffer, D.V. (2015). Viral vectors for gene therapy: translational and clinical outlook. Annu. Rev. Biomed. Eng. *17*, 63–89.
30. Campochiaro, P.A., Lauer, A.K., Sohn, E.H., Mir, T.A., Naylor, S., Anderton, M.C., Kelleher, M., Harrop, R., Ellis, S., and Mitrophanous, K.A. (2017). Lentiviral vector gene transfer of endostatin/angiostatin for macular (GEM) degeneration. Hum. Gene Ther. *28*, 99–111.
31. Yue, J., Gou, X., Li, Y., Wicksteed, B., and Wu, X. (2017). Engineered epidermal progenitor cells can correct diet-induced obesity and diabetes. Cell Stem Cell *21*, 256–263.e4.

32. Chen, C., Akerstrom, V., Baus, J., Lan, M.S., and Breslin, M.B. (2013). Comparative analysis of the transduction efficiency of five adeno associated virus serotypes and VSV-G pseudotype lentiviral vector in lung cancer cells. Virol. J. *10*, 86.

33. An, H., Cho, D.W., Lee, S.E., Yang, Y.S., Han, S.C., and Lee, C.J. (2016). Differential cellular tropism of lentivirus and adeno-associated virus in the brain of cynomolgus monkey. Exp. Neurobiol. *25*, 48–54.

34. Holmgaard, A., Askou, A.L., Benckendorff, J.N.E., Thomsen, E.A., Cai, Y., Bek, T., Mikkelsen, J.G., and Corydon, T.J. (2017). In vivo knockout of the Vegfa gene by lentiviral delivery of CRISPR/Cas9 in mouse retinal pigment epithelium cells. Mol. Ther. Nucleic Acids *9*, 89–99.

35. Zhang, X.H., Tee, L.Y., Wang, X.G., Huang, Q.S., and Yang, S.H. (2015). Off-target effects in CRISPR/Cas9-mediated genome engineering. Mol. Ther. Nucleic Acids *4*, e264.

36. Fruman, D.A., and O'Brien, S. (2017). Cancer: a targeted treatment with off-target risks. Nature *542*, 424–425.

37. White, M.K., Kaminski, R., Young, W.B., Roehm, P.C., and Khalili, K. (2017). CRISPR editing technology in biological and biomedical investigation. J. Cell. Biochem. *118*, 3586–3594.

38. Wu, Y., Zhou, H., Fan, X., Zhang, Y., Zhang, M., Wang, Y., Xie, Z., Bai, M., Yin, Q., Liang, D., et al. (2015). Correction of a genetic disease by CRISPR-Cas9-mediated gene editing in mouse spermatogonial stem cells. Cell Res. *25*, 67–79.

39. Bakondi, B., Lv, W., Lu, B., Jones, M.K., Tsai, Y., Kim, K.J., Levy, R., Akhtar, A.A., Breunig, J.J., Svendsen, C.N., and Wang, S. (2016). In vivo CRISPR/Cas9 gene editing corrects retinal dystrophy in the S334ter-3 rat model of autosomal dominant retinitis pigmentosa. Mol. Ther. *24*, 556–563.

40. Platt, R.J., Chen, S., Zhou, Y., Yim, M.J., Swiech, L., Kempton, H.R., Dahlman, J.E., Parnas, O., Eisenhaure, T.M., Jovanovic, M., et al. (2014). CRISPR-Cas9 knockin mice for genome editing and cancer modeling. Cell *159*, 440–455.

41. Liao, H.K., Hatanaka, F., Araoka, T., Reddy, P., Wu, M.Z., Sui, Y., Yamauchi, T., Sakurai, M., O'Keefe, D.D., Núñez-Delicado, E., et al. (2017). In vivo target gene activation via CRISPR/Cas9-mediated trans-epigenetic modulation. Cell *171*, 1495–1507.e15.

42. Kim, K., Park, S.W., Kim, J.H., Lee, S.H., Kim, D., Koo, T., Kim, K.E., Kim, J.H., and Kim, J.S. (2017). Genome surgery using Cas9 ribonucleoproteins for the treatment of age-related macular degeneration. Genome Res. *27*, 419–426.

43. Davar, D., Tarhini, A., and Kirkwood, J.M. (2011). Adjuvant therapy: melanoma. J. Skin Cancer *2011*, 274382.

44. Hirayama, M., Tsubota, K., and Tsuji, T. (2015). Bioengineered lacrimal gland organ regeneration in vivo. J. Funct. Biomater. *6*, 634–649.

OMTN, Volume *12*

Supplemental Information

CRISPR/Cas9-Mediated Treatment Ameliorates the Phenotype of the Epidermolytic Palmoplantar Keratoderma-like Mouse

Xiao-Rui Luan, Xiao-Ling Chen, Yue-Xiao Tang, Jin-Yan Zhang, Xiang Gao, Hai-Ping Ke, Zhao-Yu Lin, and Xian-Ning Zhang

SUPPLEMENTAL INFORMATION

Supplemental Figures

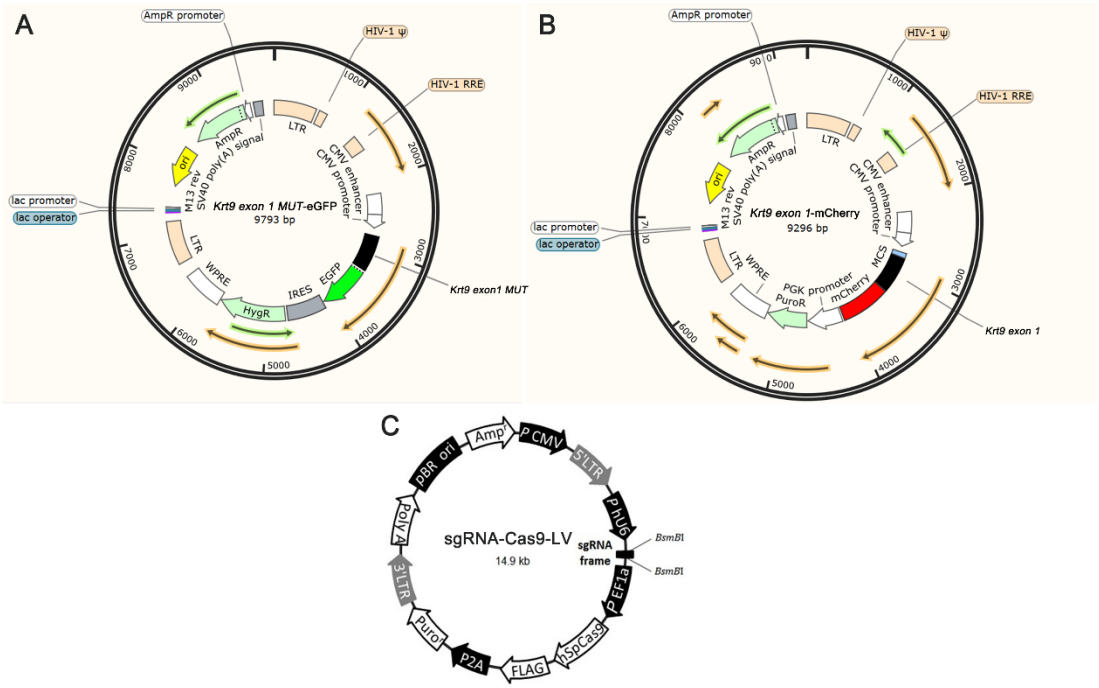

Figure S1. Constructed Vectors Used. (A, B) Diagrams of two plasmids used to establish the HeLa Hez cell line which stably expressed both *Krt9 exon1*-eGFP and *Krt9 exon1 MUT*-mCherry. (C) Diagram of LV delivery system for CRISPR-Cas9. Cas9-LV, sg1-Cas9-LV, and sg2-Cas9-LV all had the FLAG-expressing frame. While Cas9-LV had no sgRNA frame, sg1-Cas9-LV and sg2-Cas9-LV each had a different sgRNA frame.

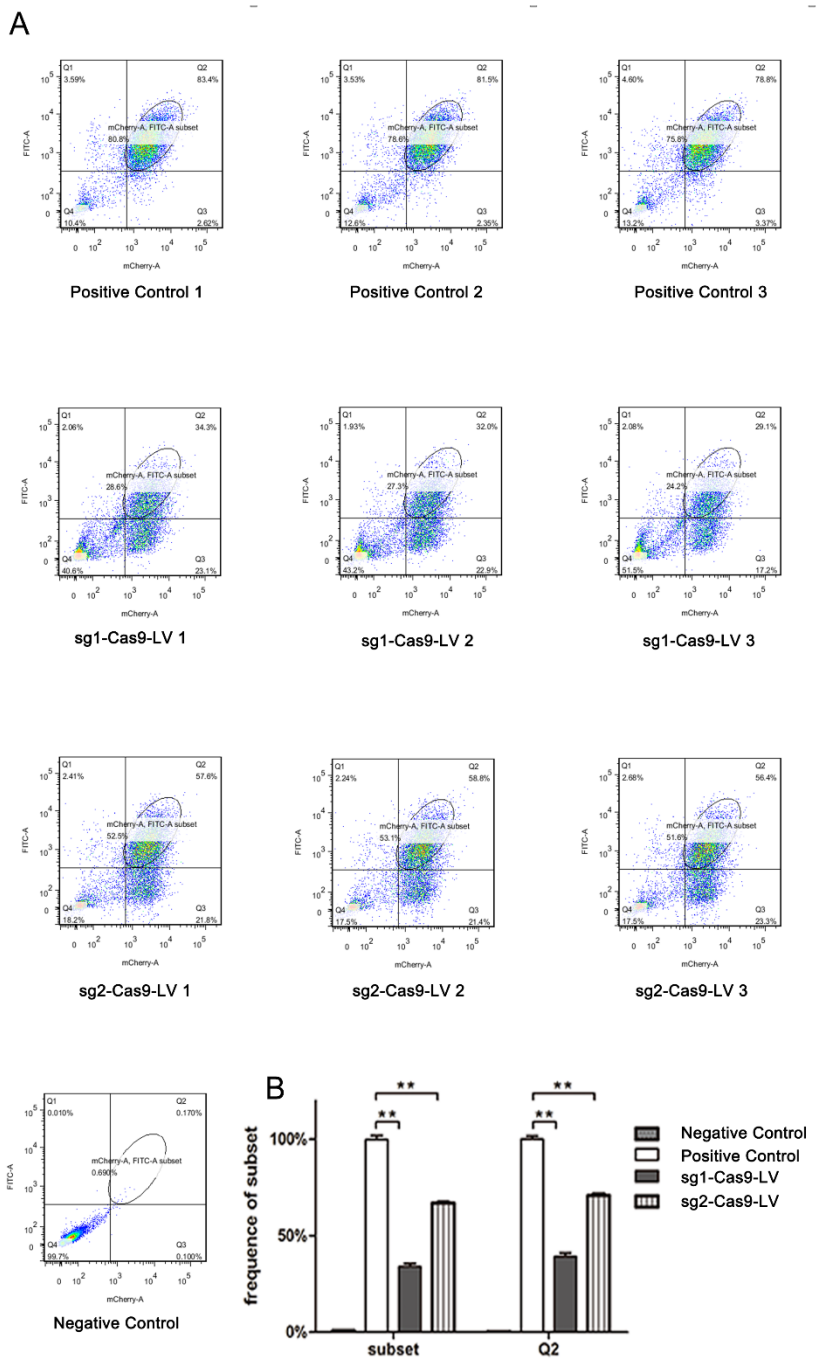

Figure S2. Flow Cytometric Analysis of Efficacy of CRISPR/Cas9 System. (A) FACs of HeLa Hezcells; circle and Q2 are subsets of cells withmCherry and eGFP fluorescence. The HeLa Hez cells were treated with different LVs. (B) Analyses of subset (circled) and Q2. 10,000 cells were collected from each sample(mean ± SEM; n=3; **P<0.01). Each experiment was repeated at least three times.

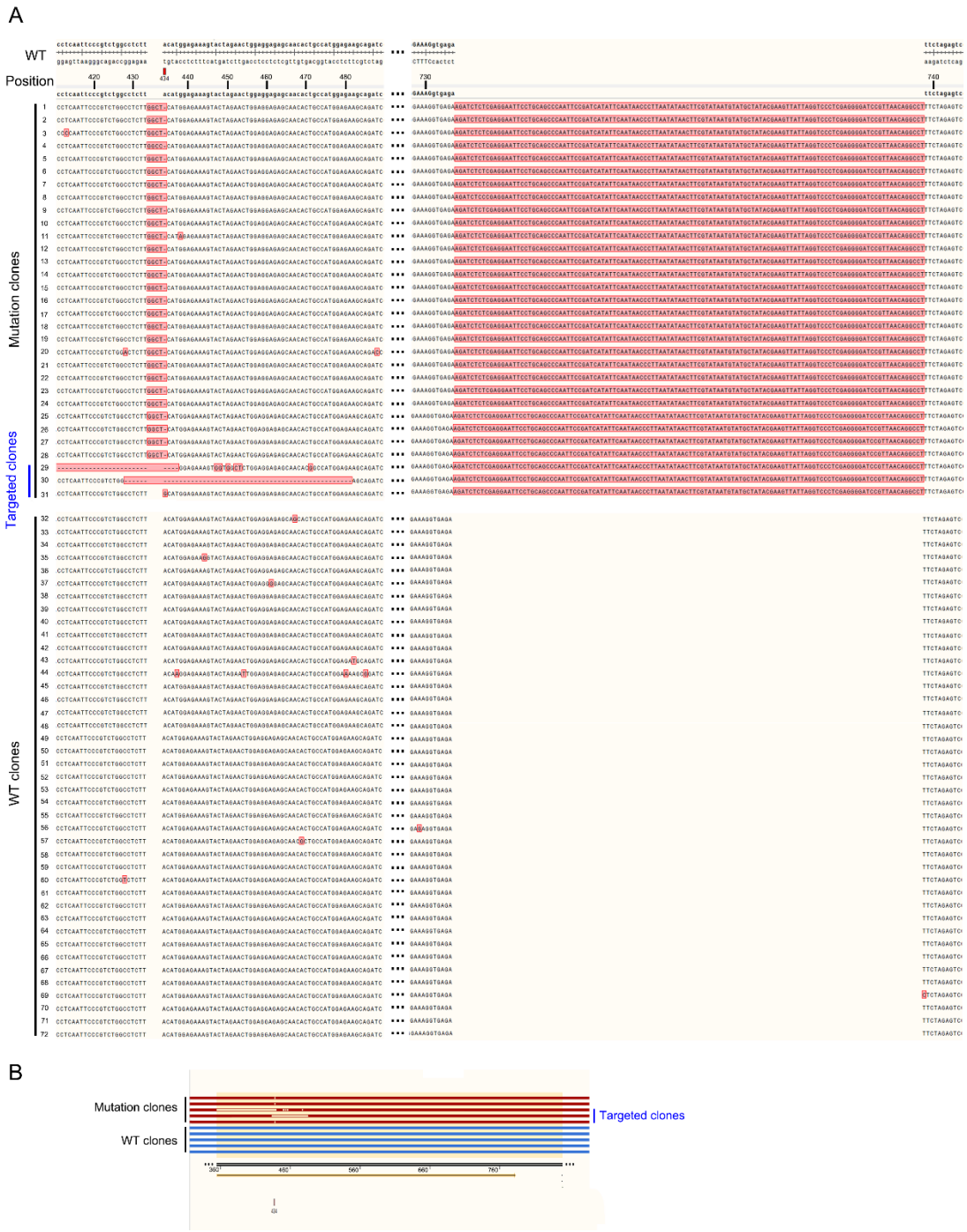

Figure S3. Sanger Sequencing Analysis of T-A Clones. (A, B) *Krt9*/c.434delAinsGGCT was the mutation site. As the KI-*Krt9* mice had other bases (GGCT) inserted within exon 1 of *Krt9*, these bases could be identified bySanger sequencing. Sequencing analyses of a total of 72 clones after sg1-Cas9-LV treatment revealed 31 mutated clones and 41 wild-type clones. Three clones with the mutatedallele were targeted by sg1-Cas9-LV.

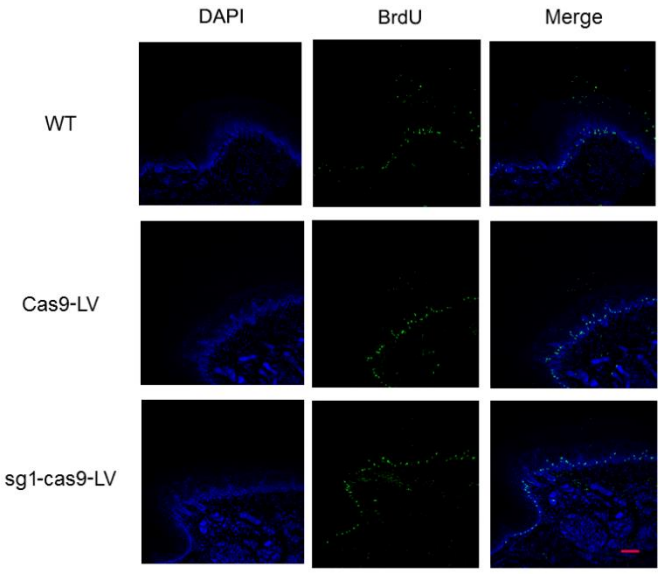

Figure S4. Immunofluorescence Against BrdU. IF staining against BrdUindicated amelioration in the epidermis of pads after sg1-Cas9-LV treatment. Scale bar, 50μm.

Supplemental Tables

Table S1. List of Predicted Top 49Potential Off-target Sites

	Sequence	Locus	Gene
1	CAGTCTGGCCTCTTGGCTCCCAG	chr16: +90882305	*Eva1c*
2	CCATCTGCCCTCTTGGCTCTGGG	chr14: +25613172	*Zmiz1*
3	GCGTCTGGCTTCTTGGCTCTAGG	chr9: +111451036	*Dclk3*
4	CAGTTTGCCTTCTTGGCTCAAAG	chr17: +8690449	*Pde10a*
5	TCCTCTGGCCTCATGGCTCACAG	chr5: +35367777	
6	CCTTCTGGCATCTTGGATCATAG	chr1: -135242443	
7	TCCTCTACCCTCTTGGCTCATGG	chr5: -35726673	*Sh3tc1*
8	CTGTCTTCCATCTTGGCTCAAGG	chr5: -142554011	
9	CCCTTTTGCTTCTTGGCTCAGAG	chr13: -40573456	
10	CATTCTGTTCTCTTGGCTCAGAG	chr17: +81953655	
11	CCTTACGACCTCTTGGCTCACAG	chr6: -56055534	
12	CCTACAGTCCTCTTGGCTCATGG	chr18: -5507756	*Gm10125*
13	CTGTTTGGCTACTTGGCTCATAG	chr1: -141190474	
14	CCCTCTGGCATCTTAGCTCAGAG	chr2: -91136498	*Mybpc3* (exonic)
15	CCCTCTTGCCTCTTGGCTTAAGG	chr5: +45434088	*Qdpr* (exonic)
16	CCTCCTGGCTGCTTGGCTCACAG	chr12: -77928545	
17	CCATCTGCCTACTTGGCTCATAG	chr18: +10503415	*Greb1l*
18	CATTCTGTCCTTTTGGCTCACAG	chr6: -148197489	*Ergic2*
19	GTCTCTGGCCTCTTGGCTCTGGG	chr4: -124255444	
20	CAGACTGCCCTCTTGGCTCCAAG	chr11: -95402645	
21	CTGGCTGTCCTCTTGGCTCTAAG	chr11: +44788874	*Ebf1*
22	CCTCTTGGCCTCTTGGCTCCCAG	chr2: -181430900	*Zbtb46*
23	CAGACTGGCTTTTTGGCTCATGG	chr2: -169325990	
24	TCGTCTGCCTTCTTGGCTCTGAG	chr9: +67972906	*Vps13c* (exonic)
25	CTCTCTGGCTTCTTGGCTCCAGG	chr17: -48899189	
26	GTGGCTGGCCTCTTGGTTCACAG	chr2: -173417917	
27	GCAGCTGGCCTCTTGGGTCAGAG	chr11: +35865560	*Wwc1*
28	GGGCCTGGCCTCCTGGCTCATGG	chr17: +90027127	
29	CAGTTTTGACTCTTGGCTCAGGG	chr2: +172958569	
30	GCCCCTGGCCTCATGGCTCATAG	chr10: -68004046	*Rtkn2*
31	CGGGCTGTCCTCCTGGCTCATAG	chr9: +47096948	
32	CAGTCACCCCTCTTGGCTCAGGG	chr16: -3854315	*Zfp174*

			(exonic)
33	CCCACTTGGCTCTTGGCTCAGAG	chr2: +116705891	
34	CAGTCTTGCCTCTTAGCTCACAG	chr12: +110681716	*1700001k19Rik*
35	CGGCCCCGCCTCTTGGCTCATGG	chr13: +17786816	*Cdk13*
36	CTGTAATGCCTCTTGGCTCACAG	chr5: -112962525	*Adrbk2*
37	CCTTTTGTCCTCCTGGCTCACGG	chr5: +148511528	*Ubl3*
38	CATTCTGGCTTCTTGGTTCACAG	chr11: +95134670	
39	CAGTCTGACATCCTGGCTCAAGG	chr7: -87242684	
40	GCGTGGGGTCTCTTGGCTCATGG	chr5: +147914988	
41	CCGTGTTCCCACTTGGCTCAGAG	chr13: +35849660	*Cdyl*
42	CAGCCTGTCCTCTTGGCTTAGAG	chr12: +92172149	*Gm40598*
43	CTTCCTGGCCTCTTGGCTAAGAG	chr9: +50277419	
44	CTCTCTGTCCTCTTGGCTGAGGG	chr17: -27930058	*Anks1*
45	CGGTAAGGCCTGTTGGCTCAGAG	chr9: +62634220	
46	TCTTCTGGTCTCTTGGCTCTCGG	chr5: +114851500	
47	CCGTCTGATCTCTTAGCTCAAAG	chr15: +73789447	*Morh5*
48	TAGTCTGTCCTCTTAGCTCAGGG	chr3: -45836873	*Gm32340*
49	ACCTCTAGCCTCATGGCTCAAAG	chr6: +55004645	

Table S2. Summary of DNA Sequencing Results within the Top 10 Off-target Sites

	Sequence	Locus	Treated/Untreated
1	CAGTCTGGCCTCTTGGCTCCCAG	chr16: +90882305	0/20
2	CCATCTGCCCTCTTGGCTCTGGG	chr14: +25613172	0/20
3	GCGTCTGGCTTCTTGGCTCTAGG	chr9: +111451036	0/20
4	CAGTTTGCCTTCTTGGCTCAAAG	chr17: +8690449	0/20
5	TCCTCTGGCCTCATGGCTCACAG	chr5: +35367777	1/19
6	CCTTCTGGCATCTTGGATCATAG	chr1: -135242443	1/19
7	TCCTCTACCCTCTTGGCTCATGG	chr5: -35726673	0/20
8	CTGTCTTCCATCTTGGCTCAAGG	chr5: -142554011	0/20
9	CCCTTTTGCTTCTTGGCTCAGAG	chr13: -40573456	0/20
10	CATTCTGTTCTCTTGGCTCAGAG	chr17: +81953655	1/19